PCCP

COMMUNICATION

View Article Online
View Journal | View Issue

The UV absorption spectrum of the simplest Criegee intermediate CH_2OO†

Cite this: *Phys. Chem. Chem. Phys.*, 2014, **16**, 10438

Received 28th February 2014,
Accepted 14th April 2014

DOI: 10.1039/c4cp00877d

www.rsc.org/pccp

Wei-Lun Ting,[a] Ying-Hsuan Chen,[a] Wen Chao,[ab] Mica C. Smith[ac] and Jim Jr-Min Lin*[abd]

SO_2 scavenging and self-reaction of CH_2OO were utilized for the decay of CH_2OO to extract the absorption spectrum of CH_2OO under bulk conditions. Absolute absorption cross sections of CH_2OO at 308.4 and 351.8 nm were obtained from laser-depletion measurements in a jet-cooled molecular beam. The peak cross section is $(1.23 \pm 0.18) \times 10^{-17}$ cm^2 at 340 nm.

Ozonolysis is a major removal mechanism in the troposphere for unsaturated hydrocarbons which are emitted in large quantities from both natural and human sources. Now it is generally accepted that ozonolysis of alkenes proceeds *via* Criegee intermediates, highly reactive species postulated in 1949 by Rudolf Criegee.[1,2] In the troposphere, Criegee intermediates are involved in several important atmospheric reactions,[3] including reactions with SO_2 and NO_2,[4–7] or can be photolyzed by near UV light,[7–10] as shown for CH_2OO in (R1)–(R4).

$$C_2H_4 + O_3 \rightarrow CH_2OO + H_2CO \quad (R1)$$

$$CH_2OO + SO_2 \rightarrow SO_3 + H_2CO \quad (R2)$$

$$CH_2OO + NO_2 \rightarrow NO_3 + H_2CO \quad (R3)$$

$$CH_2OO + h\nu \rightarrow O(^1D) + H_2CO \quad (R4)$$

The formation of SO_3 and NO_3, as in (R2) and (R3), plays an important role in atmospheric chemistry,[11,12] including aerosol and cloud formation. The formation of $O(^1D)$, as in (R4), will result in OH formation through (R5).

$$O(^1D) + H_2O \rightarrow 2OH \quad (R5)$$

Because CH_2OO absorbs strongly at wavelengths longer than 300 nm,[7–9] tropospheric photolysis of CH_2OO would be quite efficient with an effective photolysis lifetime on the order of 1 second.[8] As a result, the OH formation of (R4) + (R5) may contribute significantly to the atmospheric OH concentrations.

Despite their importance, the direct detection of Criegee intermediates was not realized until recently.[4,13] Welz *et al.*[4] reported an efficient way to prepare Criegee intermediates. For example, CH_2OO can be prepared *via* (R6) + (R7a).

$$CH_2I_2 + h\nu \rightarrow CH_2I + I \quad (R6)$$

$$CH_2I + O_2 \rightarrow CH_2OO + I \quad (R7a)$$

Welz *et al.*[4] also demonstrated the direct detection of CH_2OO by using vacuum UV photoionization mass spectrometry. The parent ion $CH_2O_2^+$ was observed when the photon energy exceeded the ionization energy of CH_2OO (10.0 eV); other isomers like dioxirane and formic acid were excluded due to their different ionization energies.[4] At low pressure, the yield of (R7a) is close to unity,[14,15] while the adduct formation (R7b) may dominate at near atmospheric pressures.[14]

$$CH_2I + O_2 + M \rightarrow ICH_2OO + M \quad (R7b)$$

The kinetics of CH_2OO reactions with SO_2 and NO_2 were investigated by Welz *et al.*[4] and by Stone *et al.*[5] by observing the disappearance of CH_2OO and by detecting the H_2CO products, respectively. The rate coefficients of these reactions were found to be unexpectedly rapid and imply a substantially greater role of Criegee intermediates in models of tropospheric sulfate and nitrate chemistry.

Beames *et al.*[8] recorded the UV spectrum of CH_2OO through observing its depletion in a molecular beam upon laser irradiation (an action spectrum). Based on their laser pulse energy and spot size, Beames *et al.*[8] roughly estimated the peak absorption cross section to be 5×10^{-17} cm^2 (at 335 nm with FWHM ~40 nm). Lehman *et al.*[10] measured the angular and velocity distributions of the $O(^1D)$ photoproduct arising from UV excitation of CH_2OO in the 300–365 nm range. From the observed

[a] *Institute of Atomic and Molecular Sciences, Academia Sinica, Taipei 10617, Taiwan*
[b] *Department of Chemistry, National Taiwan University, Taipei 10617, Taiwan*
[c] *Department of Chemistry, University of California at Berkeley, Berkeley, CA 94720, USA*
[d] *Department of Applied Chemistry, National Chiao Tung University, Hsinchu 30010, Taiwan. E-mail: jimlin@gate.sinica.edu.tw*

† Electronic supplementary information (ESI) available. See DOI: 10.1039/c4cp00877d

anisotropic angular distribution ($\beta \cong 0.97$), the authors concluded that the orientation of the transition dipole moment reflects the $\pi^* \leftarrow \pi$ character of the electronic transition associated with the COO group. The significant anisotropy of the photofragments also indicates that the dissociation is faster than rotation.

Su *et al.*[16] reported an infrared (IR) absorption spectrum of CH_2OO. By comparing their experimental results with high-level *ab initio* calculations, the authors concluded that the observed vibrational frequencies are more consistent with a zwitterion structure rather than a diradical structure. With IR detection, the same group[17] found that the self-reaction of CH_2OO is extremely fast, with a rate coefficient of $(4 \pm 2) \times 10^{-10}$ cm^3 s^{-1}, which reflects a unique property of the zwitterionic character.

Sheps[7] used a cavity-enhanced technique to measure the UV absorption spectrum of CH_2OO and observed significant vibrational structures at the long wavelength side of the absorption band. Moreover, the absorption spectrum[7] differs significantly from the action spectrum reported by Beames *et al.*[8] Sheps' argument[7] is the following: "*The difference between the absorption and action spectra likely arises from excitation to long-lived* $\tilde{B}$ $(^1A')$ *vibrational states that relax to lower electronic states by fluorescence or nonradiative processes, rather than by photodissociation.*" However, the measurement of the photoproduct anisotropy[10] indicates that the photodissociation is faster than rotation which is in the picosecond time scale. Thus, the slower fluorescence process cannot compete with the fast dissociation. Furthermore, there is no theoretical evidence for the nonradiative processes. To investigate the source of this difference, we re-investigate the UV spectrum of CH_2OO using two new methods.

CH_2OO was prepared in a pulse-photolysis cell following the well-established method of CH_2I_2/O_2 photolysis.[4,16] CH_2I_2 mixed with O_2 and N_2 was photolyzed at 248 nm (KrF excimer laser); transient absorption spectra were recorded using a gated intensified CCD camera (1 μs gate width) after the probe light was dispersed using a grating monochromator[19,20] (see ESI† for the experimental details). Fig. 1a shows examples of the transient absorption spectra. In Fig. 1a the most significant feature is a strong and broad absorption band peaked at ~340 nm which showed up quickly upon photolysis and decayed with time. In addition, depletion of the CH_2I_2 precursor near 290 nm and formation of IO with distinct peaks near 430 nm were clearly observed, especially at long delay times.

Under our experimental conditions, CH_2OO reacted quickly with itself[17] and with I atoms to form H_2CO, O_2, and IO. Because H_2CO and O_2 absorb rather weakly, the transient spectra at long delay times mainly consist of the absorption changes of CH_2I_2 (depletion) and IO (formation). Since the spectra of CH_2I_2 and IO are very different, their contributions to the transient absorption spectra can be extracted and removed (see ESI† for details). The remaining spectra are shown in Fig. 2a. Consistent with ref. 14, we did not observe significant difference in the CH_2OO yield for different O_2 mixing ratios. The identical shape of these spectra under various experimental conditions (delay times, laser fluences, and O_2 pressures) strongly suggests that the spectral carrier is a single species. Based on the high yield of CH_2OO from the CH_2I_2/O_2 photolysis at low pressure,[14,15] it is most reasonable to assign the spectral carrier to CH_2OO (see below for discussion on the pressure dependence). If another absorbing species contributes significantly to these spectra, this species must exhibit kinetic behavior similar to that of CH_2OO.

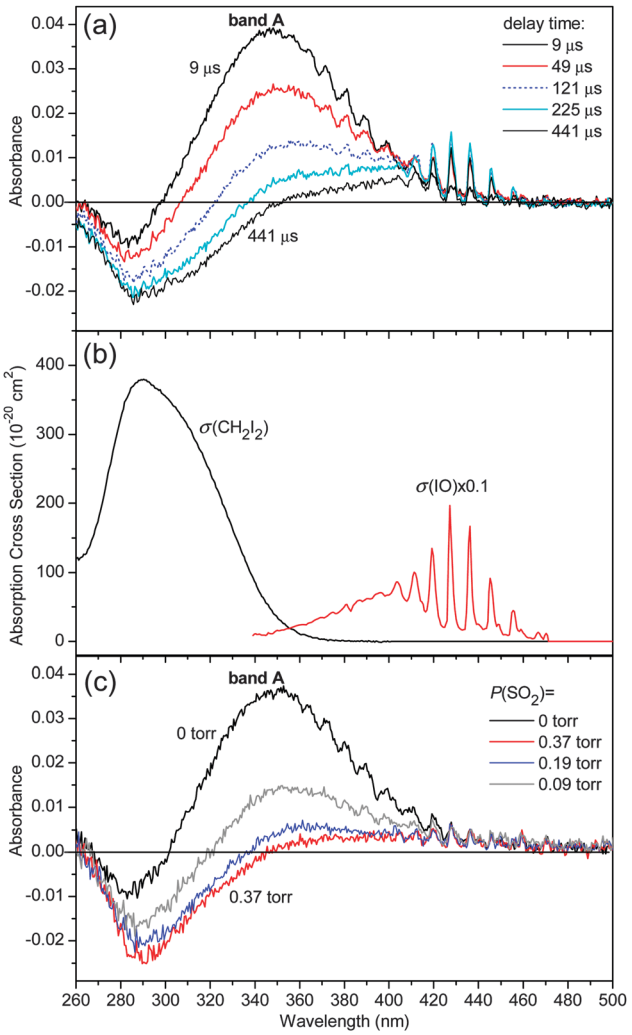

Fig. 1 (a) Examples of the transient absorption spectra. The $[CH_2I_2]_0$, $[O_2]_0$ and the total number density n_{total} (N_2 balance) are 1.6×10^{15}, 3.4×10^{17} and 2.0×10^{18} cm^{-3}, respectively. The depletion of CH_2I_2 (<10% of $[CH_2I_2]_0$) results in negative absorbance peaked at ~290 nm. The broad and strong absorption band peaked at ~340 nm (band A) is most likely due to CH_2OO, which is short-lived. At longer delay times, the formation of IO gives sharp peaks in the 410–460 nm range. (b) Published spectra of CH_2I_2 and IO.[18] (c) Examples of transient absorption spectra at different SO_2 concentrations. It is clear that the intensity of band A decreases at higher SO_2 concentrations. $[CH_2I_2]_0$, $[O_2]_0$, and n_{total} are 1.3×10^{15}, 1.6×10^{18}, 3.3×10^{18} cm^{-3}, respectively; delay time = 10.6 μs.

It is known that CH_2OO reacts quickly with SO_2 ($k_2 \sim (3\text{–}4) \times 10^{-11}$ cm^3 s^{-1}).[4,5] We utilized this kinetic signature of CH_2OO to examine the spectral carrier of band A. As shown in Fig. 1c, it is clear that the intensity of band A decreases at higher SO_2 concentrations. Because the absorption cross sections of SO_2, H_2CO and SO_3 in the 316–450 nm range are much smaller

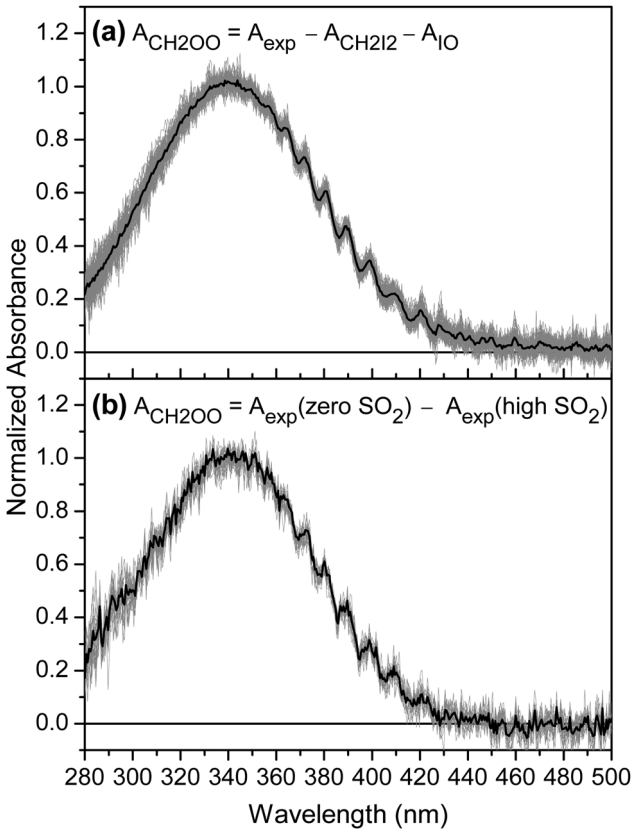

Fig. 2 (a) Background-corrected height-normalized spectra of CH_2OO. The variation of the experimental parameters includes combinations of delay time (2–50 μs) and gas composition (O_2 percentage: 17–99%, N_2 balance), total pressure (7.5–100 Torr), laser fluence (8–16 mJ cm^{-2}), *etc.* A total of 99 spectra (gray lines) and their average (black line) are plotted. (b) Height-normalized spectra of CH_2OO obtained by subtracting the experimental spectra at different SO_2 concentrations. A total of 24 spectra (gray lines) and their average (black line) are plotted. Delay time: 6.5–50 μs; $[SO_2]$: $2.9 \times 10^{15} - 1.2 \times 10^{16}$ cm^{-3}.

($<1 \times 10^{-19}$ cm^2) than those of CH_2OO (peak cross section $>1 \times 10^{-17}$ cm^2),[8] the differences between the spectra of Fig. 1c should be mostly due to the absorption of CH_2OO. The height-normalized curves of such difference spectra are shown in Fig. 2b. The good agreement between Fig. 2a and b confirms the above assignment.

When O_2 was absent in the photolysis cell, the absorption of CH_2I was present and band A could not be observed. With the published absorption cross sections of CH_2I,[21] the initial number density of CH_2I can be estimated. Under the high O_2 pressures used, CH_2I reacted with O_2 within a few microseconds.[5,7,14,15] Therefore the number density of CH_2OO can be estimated based on the published quantum yield of (R7a) ($\Phi_{CH_2OO} = 86\%$ at 11 Torr).[14] From the estimated number density and the observed absorbance of CH_2OO, its absolute peak cross section can be deduced to be $(1.26 \pm 0.25) \times 10^{-17}$ cm^2 at 340 nm. The overall error bar is estimated to be ±20% mostly due to the uncertainty in Φ_{CH_2OO}[14,15] (see ESI† for details).

In Fig. 2a we can see that the shape of band A does not depend on the total pressure in the range of 8–100 Torr. This observation excludes the contribution of ICH_2OO because its formation is a termolecular process which has strong pressure dependence.[14,15] At higher pressures (100 Torr $< P <$ 760 Torr), the yield of CH_2OO was found to decrease with pressure (see Table S1 (ESI†) for a typical example) and an additional (weaker) absorption band was observed at $\lambda < 290$ nm, indicating the formation of a new species (likely ICH_2OO).[21,22] The absorption of ICH_2OO seems to be much weaker than that of CH_2OO, such that the change in spectral shape (not including the yield) with pressure is not very obvious.

The IO peaks are absent in short delay times while the absorption of CH_2OO is very significant, indicating that IO is not a primary product. Based on our signal-to-noise ratio, we further constrain the primary IO yield to be less than 1%, resolving some debate among published results.[23–26] The formation of IO is likely due to (R8).[5,14]

$$CH_2OO + I \rightarrow H_2CO + IO \qquad (R8)$$

Detailed kinetic analysis is beyond the scope of this paper and will be published elsewhere.

To further quantify the absolute value of the absorption cross section of CH_2OO, we measured the depletion of CH_2OO in a molecular beam upon laser irradiation at 308.4 and 351.8 nm. CH_2OO was detected using a quadrupole mass spectrometer equipped with an electron impact ionizer. This method[27–29] has been demonstrated to be efficient in determining the photodissociation cross section of a species in a mixture without the knowledge of its concentration. Under our experimental conditions, the number of molecules N after laser irradiation can be described by eqn (1).

$$\frac{N}{N_0} = e^{-I\sigma\phi} \quad \frac{\Delta N}{N_0} = 1 - e^{-I\sigma\phi} \qquad (1)$$

Where N_0 is the number of molecules before the laser irradiation, I is the laser fluence in photons per cm^2, σ is the absorption cross section in cm^2, ϕ is the dissociation quantum yield and $\Delta N = N_0 - N$. For CH_2I_2, the excitations at 351.8 and 308.4 nm correspond to repulsive (unbound) excited states which dissociate in picosecond time scales,[30–32] resulting in 100% dissociation ($\phi = 1$).

Fig. 3a shows the arrival-time profiles of CH_2OO at various laser fluences at 308.4 nm. Fig. 3b shows the corresponding saturation curve. A nice fit of eqn (1) to the experimental data indicates that the measurement corresponds to a single species (or multiple species having the same cross section, which is unlikely). The results at 351.8 nm are similar (see ESI†). The complete depletion of CH_2OO indicates that its dissociation yield is unity. The absolute cross section of CH_2OO can be obtained by comparing its saturation curve with that of CH_2I_2, for which the cross section is known. A summary of the cross section measurement is shown in Table 1.

With the absolute cross sections of CH_2OO (Table 1), we may set the spectra of Fig. 2 on the absolute scale. However, we need to consider the temperature effect of the absorption cross sections because the temperature of the molecular beam is lower than room temperature. Since the cross section of CH_2I_2

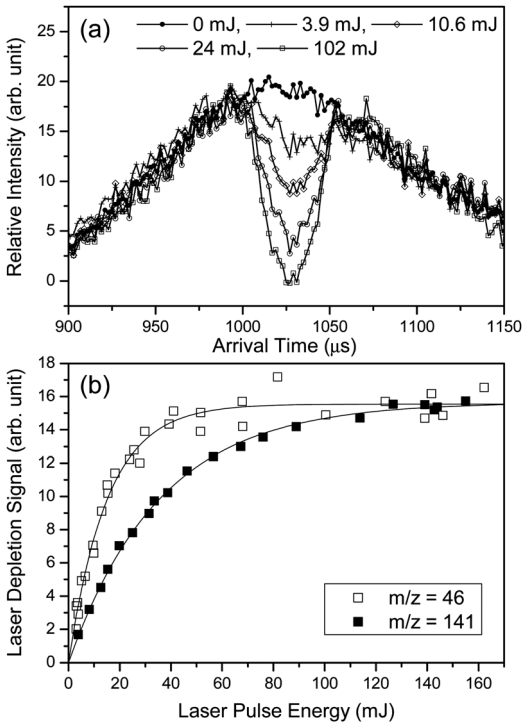

Fig. 3 (a) Arrival-time profiles of CH_2OO at various laser fluences at 308.4 nm. The parent ion of CH_2OO was detected at m/z = 46 amu. (b) Saturation curve for the laser depletion of CH_2OO (m/z = 46) and CH_2I_2 (m/z = 141, CH_2I^+, a daughter ion of CH_2I_2) at 308.4 nm. The x-axis is the laser pulse energy which is proportional to the laser fluence. The lines are the fit of eqn (1). The nice fit indicates that the laser depletion experiments are single-photon processes.

Table 1 Summary of the cross section measurements of CH_2OO in a jet-cooled molecular beam

Wavelength (nm)	$\frac{\sigma\phi(CH_2OO)}{\sigma\phi(CH_2I_2)}$	$\sigma(CH_2I_2)^b$ (cm^2)	$\sigma(CH_2OO)$ (cm^2)
308.4	2.52 ± 0.28^a	3.21×10^{-18}	$(8.09 \pm 0.90) \times 10^{-18}$
351.8	47.6 ± 5.2	$\leq 2.54 \times 10^{-19}$	$\leq (1.21 \pm 0.13) \times 10^{-17}$

[a] The error bar is 2 standard deviation. [b] Average values of ref. 33 and 34 at T = 273 K. The temperature dependence of the UV absorption cross section of CH_2I_2 is very weak at 308.4 nm, but moderate at 351.8 nm.[34] The actual cross section at 351.8 nm would be smaller for CH_2I_2 in a jet-cooled molecular beam.

at 308.4 nm does not change with temperature,[33,34] we can use the near-room-temperature value for the cross section of CH_2I_2 in a molecular beam. The UV absorption band of CH_2OO can be assigned to the intense $\tilde{B} \leftarrow \tilde{X}$ transition[8,22] which is analogous to the Hartley band of O_3. The cross section of the O_3 Hartley band has a quite weak temperature dependence.[18,35] The peak cross section (at 254 nm) of O_3 increases by $\sim$1.5% when the temperature decreases from 293 K to 203 K. For the main region of the Hartley band (215–288 nm, 1×10^{-18} $cm^2 < \sigma < 1.1 \times 10^{-17}$ cm^2), the temperature effect is within 5% (203–293 K).[18,35] Similarly, it is expected that the temperature dependence of the CH_2OO cross sections is weak near the peak. Therefore, we choose the cross section at 308.4 nm to scale the average spectra of Fig. 2 and to plot the scaled spectra in Fig. 4. We believe that the SO_2 scavenging method would give a more reliable spectrum of CH_2OO (see Table S3 (ESI†) for numerical values) while the result of the self-reaction method is very similar. The peak value of the scaled spectrum is $(1.23 \pm 0.18) \times 10^{-17}$ cm^2 at 340 nm. We assume an error bar of $\pm$15% to include possible variations due to the temperature effect. This value is consistent with the peak cross section of $(1.26 \pm 0.25) \times 10^{-17}$ cm^2 obtained in the transient absorption experiment of this work based on the estimated CH_2OO number density.

Previous UV absorption[7] and action spectra[8] of CH_2OO exhibit significant differences. Beames *et al.*[8] measured the laser depletion of CH_2OO in a similar molecular beam and obtained an action spectrum of CH_2OO. However Beames *et al.*[8] only estimated the laser fluence from their laser (a dye laser) pulse energy and spot size. The beam spot of a dye laser is usually highly non-uniform. Without using a laser beam profiler, it is difficult to quantify the actual laser fluence. Beames *et al.*[8] might underestimate their laser fluence and thus overestimate the CH_2OO cross section. In this work, we utilized a reference molecule to effectively calibrate the laser fluence and to cancel the effect of non-uniform laser spot.[36] Therefore, our results should be more accurate.

Fig. 4 compares our results with those of Sheps[7] and Beames *et al.*[8] The scaled spectrum of Beames *et al.*[8] is weaker at $\lambda \geq$ 360 nm. The temperature effect may be one possible reason for this difference. While the intense Hartley band of O_3 has a rather weak temperature dependence, the weak Huggins band or the long-wavelength tail of the Hartley band (310–380 nm) has very strong temperature dependence (smaller cross sections at lower temperatures).[18,35] If the temperature dependence of the CH_2OO cross sections at $\lambda \geq$ 360 nm is as strong as that of the Huggins band of O_3, this may explain why the spectrum of Beames *et al.*[8] is weaker in this wavelength range. Another possibility mentioned by Sheps[7] is a decrease in the dissociation yield at long wavelengths. Although this might explain the discrepancy between the absorption and action spectra, it is inconsistent with the product anisotropy measurement by Lehman *et al.*[10] which shows that the UV photodissociation of CH_2OO is faster than its rotation ($\sim$picosecond). Thus, a non-unity dissociation yield would require a fast process that can compete with photodissociation. Fluorescence is too slow to fulfill this condition. Other fast non-radiative processes are unlikely but cannot be fully ruled out at this moment. More evidence and investigations are needed.

Sheps[7] used a newly-built cavity-enhanced absorption spectrometer to measure the transient absorption spectra of the CH_2I_2/O_2 photolysis system. Sheps[7] determined the absolute CH_2OO spectrum based on the measured CH_2I spectrum (when O_2 was absent) and an estimated (90 $\pm$ 10)% yield of transforming CH_2I to CH_2OO at 5 Torr. Qualitatively, the shape of Sheps' spectrum[7] is similar to ours, particularly the structures at the long-wavelength side (the peak positions are matched). However, the short-wavelength side of Sheps' spectrum[7] decays much faster than that in this work. Furthermore, the reported peak cross section and position of the CH_2OO spectrum by

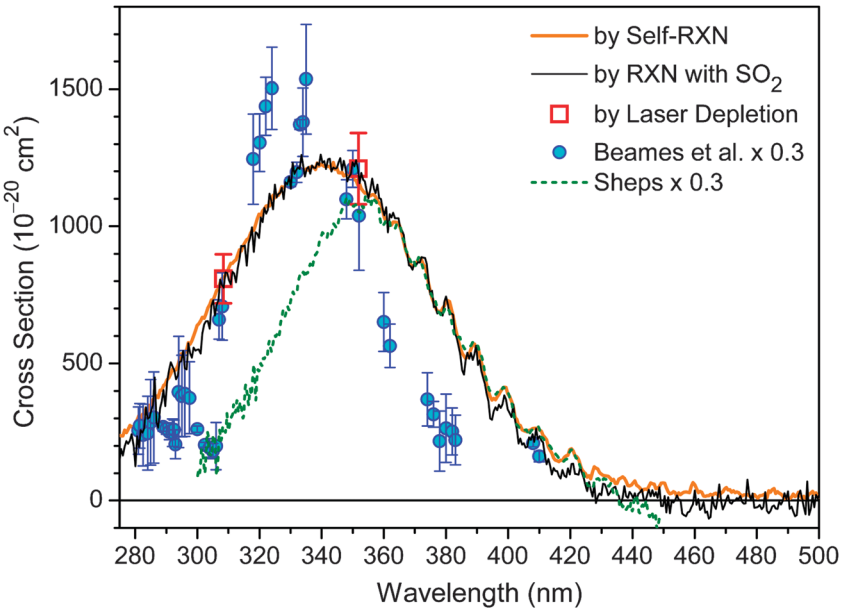

Fig. 4 Absorption spectrum of CH_2OO. The thick orange and thin black lines are the average curves of Fig. 2a and b, respectively. For the thin black line (numerical values can be found in ESI†), the absorbance due to the reacted SO_2 has been removed, based on the mass balance of (R2) (see ESI†). Square symbols are the absolute cross sections from the molecular beam-laser depletion measurements (Table 1). The black and orange lines are scaled to match the absolute cross section at 308.4 nm. The results of Sheps[7] and Beames *et al.*[8] are scaled by a factor of 0.3 for easier comparison. The temperature of the photolysis cell was 295 K. The molecular beams of this work and Beames *et al.*[8] were jet-cooled (estimated rotational temperature ~10 K).

Sheps[7] [$(3.6 \pm 0.9) \times 10^{-17}$ cm^2 at 355 nm] are different from our values. The source of the discrepancies is not clear. It might arise from the complexity of the cavity-enhanced measurement.

There are at least 7 vibrational peaks observable on the long-wavelength side of the UV absorption band of CH_2OO (Fig. 2 and 4). The widths of these vibrational peaks are significantly wider than the instrument resolution of ~2 nm. Similar structures have been reported by Sheps[7] at a slightly lower resolution and signal-to-noise ratio. The positions of the most well-defined peaks are 363.7, 372.0, 380.7, 389.2, 399.0, 409.3, 420.5 nm (27495, 26882, 26267, 25694, 25063, 24432, 23781 cm^{-1}). The average peak separation is about 620 cm^{-1}. Analogous to the Huggins band of O_3, these vibrational structures may arise from some periodic motions on the excited potential energy surface, most likely the $\tilde{B}(^1A')$ surface. The widths of the vibrational peaks may originate from congested vibrational structures (vibrational modes involving O–O stretching and C–O–O bending)[22] or rotational contours at room temperature. For the O_3 Huggins band, the widths of the vibrational peaks become narrower at low temperatures.[18,35] It will be interesting to see how the peak structures change at lower temperatures for CH_2OO.

In summary, more accurate UV absorption cross sections of the simplest Criegee intermediate CH_2OO are reported. The peak cross section is determined to be $(1.23 \pm 0.18) \times 10^{-17}$ cm^2 at 340 nm. This value is significantly smaller than previous reports,[7,8] implying slower photolysis rates in the atmosphere than previously expected. Nonetheless, this intense absorption band of CH_2OO overlaps well with the incoming solar spectrum, resulting in efficient photolysis of this Criegee intermediate. The clear vibrational structures on the long-wavelength side of the CH_2OO spectrum provide a fingerprint feature for spectroscopic identification of this elusive intermediate.

Acknowledgements

This work was supported by Academia Sinica and Ministry of Science and Technology, Taiwan (NSC100-2113-M-001-008-MY3). The authors thank Miss Shu-Yi Meng for assistance in data acquisition and Profs Yuan T. Lee and Yuan-Pern Lee for discussions.

References

1 R. Criegee, *Angew. Chem., Int. Ed. Engl.*, 1975, **14**, 745–752.
2 R. Criegee and G. Wenner, *Liebigs Ann. Chem.*, 1949, **564**, 9–15.
3 C. A. Taatjes, D. E. Shallcross and C. Percival, *Phys. Chem. Chem. Phys.*, 2014, **16**, 1704–1718, DOI: 10.1039/C3CP52842A.
4 O. Welz, J. D. Savee, D. L. Osborn, S. S. Vasu, C. J. Percival, D. E. Shallcross and C. A. Taatjes, *Science*, 2012, **335**, 204–207.
5 D. Stone, M. Blitz, L. Daubney, N. U. M. Howesa and P. Seakins, *Phys. Chem. Chem. Phys.*, 2014, **16**, 1139–1149, DOI: 10.1039/c3cp54391a.
6 B. Ouyang, M. W. McLeod, R. L. Jones and W. J. Bloss, *Phys. Chem. Chem. Phys.*, 2013, **15**, 17070–17075.
7 L. Sheps, *J. Phys. Chem. Lett.*, 2013, **4**, 4201–4205.
8 J. M. Beames, F. Liu, L. Lu and M. I. Lester, *J. Am. Chem. Soc.*, 2012, **134**, 20045–20048.
9 J. M. Beames, F. Liu, L. Lu and M. I. Lester, *J. Chem. Phys.*, 2013, **138**, 244307.

10 J. H. Lehman, H. Li, J. M. Beames and M. I. Lester, *J. Chem. Phys.*, 2013, **139**, 141103.
11 C. J. Percival, *et al.*, *Faraday Discuss.*, 2013, **165**, 45–73.
12 M. Boy, D. Mogensen, S. Smolander, L. Zhou, T. Nieminen, P. Paasonen, C. Plass-Dülmer, M. Sipilä, T. Petäjä, L. Mauldin, H. Berresheim and M. Kulmala, *Atmos. Chem. Phys.*, 2013, **13**, 3865–3879.
13 C. A. Taatjes, G. Meloni, T. M. Selby, A. J. Trevitt, D. L. Osborn, C. J. Percival and D. E. Shallcross, *J. Am. Chem. Soc.*, 2008, **130**, 11883–11885.
14 D. Stone, M. Blitz, L. Daubney, T. Ingham and P. Seakins, *Phys. Chem. Chem. Phys.*, 2013, **15**, 19119–19124.
15 H. Huang, A. J. Eskola and C. A. Taatjes, *J. Phys. Chem. Lett.*, 2012, **3**, 3399–3403; H. Huang, B. Rotavera, A. J. Eskola and C. A. Taatjes, *J. Phys. Chem. Lett.*, 2013, **4**, 3824.
16 Y.-T. Su, Y.-H. Huang, H. A. Witek and Y.-P. Lee, *Science*, 2013, **340**, 174–176.
17 Y.-T. Su, H.-Y. Lin, R. Putikam, H. Matsui, M. C. Lin and Y.-P. Lee, *Nat. Chem.*, 2014, DOI: 10.1038/nchem.1890.
18 S. P. Sander, J. Abbatt, J. R. Barker, J. B. Burkholder, R. R. Friedl, D. M. Golden, R. E. Huie, C. E. Kolb, M. J. Kurylo, G. K. Moortgat, V. L. Orkin and P. H. Wine, *Chemical Kinetics and Photochemical Data for Use in Atmospheric Studies, Evaluation Number 17*, JPL Publication 10-6, Jet Propulsion Laboratory, Pasadena, 2011, http://jpldataeval.jpl.nasa.gov.
19 M.-N. Su and J. J. Lin, *Rev. Sci. Instrum.*, 2013, **84**, 086106.
20 M.-N. Su and J. J. Lin, *GSTF Journal of Chemical Sciences (JChem)*, 2013, **1**, 52–57, DOI: 10.5176/2339-5060_1.1.6, ISSN: 2339-5060.
21 J. Sehested, T. Ellermann and O. J. Nielsen, *Int. J. Chem. Kinet.*, 1994, **26**, 259–272.
22 E. P. F. Lee, D. K. W. Mok, D. E. Shallcross, C. J. Percival, D. L. Osborn, C. A. Taatjes and J. M. Dyke, *Chem. – Eur. J.*, 2012, **18**, 12411–12423.
23 T. J. Gravestock, M. A. Blitz, W. J. Bloss and D. E. Heard, *ChemPhysChem*, 2010, **11**, 3928.
24 T. J. Dillon, M. E. Tucceri, R. Sander and J. N. Crowley, *Phys. Chem. Chem. Phys.*, 2008, **10**, 1540.
25 A. J. Eskola, D. Wojcik-Pastuszka, E. Ratajczak and R. S. Timonen, *Phys. Chem. Chem. Phys.*, 2006, **8**, 1416–1424.
26 S. Enami, T. Yamanaka, S. Hashimoto, M. Kawasaki, K. Tonokura and H. Tachikawa, *Chem. Phys. Lett.*, 2007, **445**, 152–156.
27 H.-Y. Chen, C.-Y. Lien, W.-Y. Lin, Y. T. Lee and J. J. Lin, *Science*, 2009, **324**, 781.
28 J. J. Lin, A. F. Chen and Y. T. Lee, *Chem. – Asian J.*, 2011, **6**, 1664.
29 B. Jin, M.-N. Su and J. J. Lin, *J. Phys. Chem. A*, 2012, **116**, 12082–12088.
30 J. Zhang, E. J. Heller, D. Huber, D. G. Imre and D. Tannor, *J. Chem. Phys.*, 1988, **89**, 3602.
31 H. F. Xu, Y. Guo, S. L. Liu, X. X. Ma, D. X. Dai and G. H. Sha, *J. Chem. Phys.*, 2002, **117**, 5722.
32 J. H. Lehman, H. Li and M. I. Lester, *Chem. Phys. Lett.*, 2013, **590**, 16–21.
33 J. C. Mössinger, D. E. Shallcross and R. A. Cox, *J. Chem. Soc., Faraday Trans.*, 1998, **94**, 1391–1396.
34 C. M. Roehl, J. B. Burkholder, G. K. Moortgat, A. R. Ravishankara and P. J. Crutzen, *J. Geophys. Res.*, 1997, **102**, 12819–12829.
35 W. Chehade, B. Gür, P. Spietz, V. Gorshelev, A. Serdyuchenko, J. P. Burrows and M. Weber, *Atmos. Meas. Tech.*, 2013, **6**, 1623–1632.
36 B. Jin, I.-C. Chen, W.-T. Huang, C.-Y. Lien, N. Guchhait and J. J. Lin, *J. Phys. Chem. A*, 2010, **114**, 4791.